J|A|C|S
ARTICLES
Published on Web 09/23/2004

Chiral Recognition of Dipeptides in a Biomembrane Model

Cecilia Bombelli,[†] Stefano Borocci,[§] Federica Lupi,[||] Giovanna Mancini,*[,†] Luisa Mannina,[⊥,▽] Anna Laura Segre,[⊥] and Stéphane Viel[⊥,▽]

Contribution from the IMC-Sezione Meccanismi di Reazione, CNR, c/o Dipartimento di Chimica, Università "La Sapienza", P. le Aldo Moro 5, Box 34, Roma 62, 00185 Roma, Centro di Eccellenza per i Materiali Innovativi Nanostrutturati per Applicazioni Chimiche, Fisiche e Biomediche, CEMIN, Dipartimento di Scienze Ambientali, Università della Tuscia, L. go dell'Università, 01100 Viterbo, Dipartimento di Chimica, Università degli Studi di Roma "La Sapienza", P. le Aldo Moro 5, Box 34, Roma 62, 00185 Roma, Istituto di Metodologie Chimiche, CNR, Via Salaria Km 29.300, 00016 Monterotondo Staz. Roma, and Dipartimento di STAAM, Università del Molise, 86100 Campobasso, Italy

Received May 21, 2004; E-mail: gmancini@uniroma1.it

Abstract: Chiral recognition of the enantiomeric couples of ditryptophan and diphenylalanine was observed by ^{1}H NMR spectroscopy in micelles formed by sodium *N*-dodecanoyl-L-prolinate. Ditryptophan showed a selective association with the *Z* domains of the amidic aggregates, whereas diphenylalanine did not show any selectivity in the association. Partition coefficients between water and aggregates were evaluated by diffusion NMR experiments. Intramolecular distances of ditryptophan isomers associated with chiral aggregates were obtained by ROESY experiments and were used as constraints in molecular mechanics calculations. From these calculations, information on the conformation of the peptides in the chiral aggregates was obtained.

Introduction

Chiral recognition in biomembrane models is of fundamental interest. In fact, the organization of biomembranes is based on molecular recognition phenomena, and the understanding of the fundamental noncovalent interactions responsible for the organization and compartmentalization of simple models, characterized by a definite chemical composition, is a first step in the comprehension of the structure and function of biomembranes. Chiral recognition is a particular aspect of molecular recognition; many components of biomembranes are chiral, and chiral recognition plays a role in the organization of biomembranes and in many functions of these self-aggregated systems. Because many molecules important to life are chiral, to clarify the noncovalent interactions responsible for chiral recognition phenomena in a biological system is of crucial importance.

Another interesting aspect of the study of chiral recognition in biomembrane models relates to the role that biomembranes may have played in the homochirality of biopolymers. One of the most intriguing problems in life sciences is the time and the mechanism of symmetry breaking. Many theories have been proposed on these topics and in the attempt to explain the amplification of a first enantiomeric imbalance to the enantiopurity of biomolecules.[1] In all theories on symmetry breaking and on enantiomeric excess amplification little attention has been paid to the possible role of biomembranes, or of simple self-aggregated systems that may have acted as primitive biomembranes. Nevertheless, it is possible that amphiphilic boundary systems, which are considered by many scientists as intimately connected to the emergence and the development of life,[2] had played a role in the history of homochirality in virtue of recognition and compartmentalization phenomena.[3]

In this context, an investigation on chiral recognition of dipeptides in chiral micellar aggregates was performed. Here we describe the observation by ^{1}H NMR of chiral discrimination of the LL/DD and LD/DL enantiomeric couples of ditryptophan (**1**) and diphenylalanine (**2**) by chiral micelles formed by sodium *N*-dodecanoyl-L-prolinate (SDP) (**3**) and the difference between homo- and heterochiral dipeptides in the interaction with the chiral aggregates.

We chose aromatic peptides because of the high affinity of aromatic amino acids for lipidic aggregates. In particular, tryptophan is known to play a role in the interaction of membrane proteins with the lipid double layer.[4] Moreover, the presence of aromatic portions in the peptide eases the NMR detection of the sites of peptide−micellar aggregate interaction.

[†] IMC-Sezione Meccanismi di Reazione, CNR.
[§] Università della Tuscia.
[||] Università degli Studi di Roma "La Sapienza".
[⊥] Istituto di Metodologie Chimiche, CNR.
[▽] Università del Molise.

(1) Avalos, M.; Babiano, R.; Cintas, P.; Jiménez, J. L.; Palacios, J. C. *Tetrahedron: Asymmetry* **2000**, *11*, 2845−2874.
(2) (a) Bachmann, P. A.; Luisi, P. L.; Lang, J. *Nature* **1992**, *357*, 57−59. (b) Menger, F. M.; Angelova, M. I. *Acc. Chem. Res.* **1998**, *31*, 789−797. (c) Ourisson, G.; Nakatani, Y. *Tetrahedron* **1999**, *55*, 3183−3190. (d) Segré, D.; Ben-Eli, D.; Deamer, D. W.; Lancet, D. *Origins Life Evol. Biosphere* **2001**, *31*, 119−145.
(3) (a) Arnett, E. M.; Thompson, O. *J. Am. Chem. Soc.* **1981**, *103*, 968−970. (b) Hitz, T.; Luisi, P. L. *Biopolym. (Pept. Sci.)* **2001**, *55*, 381−390. (c) Weissbuch, I.; Bolbach, G.; Leiserowitz, L.; Lahav, M. *Origins Life Evol. Biosphere* **2004**, *34*, 79−92.
(4) Yau, W.-M.; Wimley, W. C.; Gawrisch, K.; White, S. H. *Biochemistry* **1998**, *37*, 14713−14718.

10.1021/ja0470057 CCC: $27.50

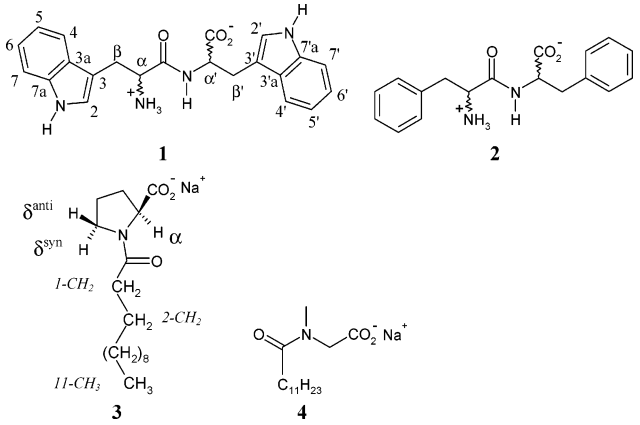

1 **2**

3

4

As a counterpart, although sodium *N*-dodecanoyl-L-prolinate is not a natural amphiphile, we have chosen it in this study because it is characterized by a high extent of organization and the interactions involved in its micellar aggregates are similar to those responsible for the aggregation and organization of the aggregates formed by natural lipids. In fact, it is known that, under aggregating conditions, the geometrical isomers (Scheme 1) of amidic surfactants form domains on the basis of their *E*/*Z* configuration.[5] Moreover, the aggregates formed by SDP are able to discriminate enantiomers.[6]

Results and Discussion

The aromatic regions of the ^{1}H NMR spectra of each diastereoisomer of 20 mM ditryptophan in D_2O micellar solutions of 94 mM SDP in 100 mM phosphate buffer are reported in Figure 1. It can be observed that the spectra of the enantiomers are different for both homochiral and heterochiral isomers, because the diastereomeric interactions with the chiral aggregates yield different chemical shifts for some of the resonances of enantiomeric **1**. The same observation holds also for the enantiomeric couples of **2**, as can be observed in Figure 2. Therefore, in the presence of the micellar chiral aggregates, we can recognize by NMR the LL/DD and the DL/LD enantiomers of both dipeptides.

The signals of the two amino acidic residues of **1** were assigned according to the unequivocal assignment of the α and α′ proton signals of LL-**1** in CD_3OD reported in the literature;[7] because of the strong spectral similarity, the α and α′ proton signals of DD-**1**, DL-**1**, and LD-**1** were assigned accordingly. 2D NMR experiments, performed on each diastereomer of **1** in the presence of a buffered micellar chiral solution of SDP, allowed all NMR signals to be assigned, as shown in Figure 1 and reported in Table 1. ^{1}H and ^{13}C resonances of ditryptophan isomers (3.8 mM) in the presence of SDP (94 mM) as well as those of the LL and LD isomers in 100 mM D_2O phosphate buffer are available as Supporting Information (Tables 1S−6S).[8]

Note that in the presence of micellar chiral aggregates NMR chiral discrimination is still observable in the NMR spectra of the racemic mixtures of **1** and **2**, as clearly shown in Figure 3,

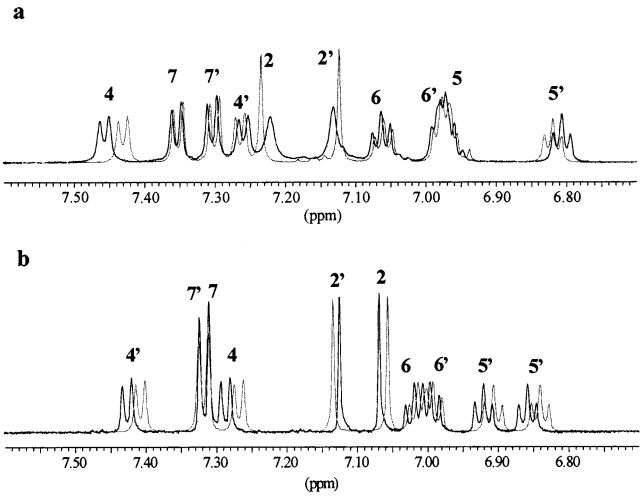

Figure 1. Comparison of the aromatic regions of the 600.13 MHz ^{1}H NMR spectra of 20 mM **1** enantiomers in 94 mM SDP: (a) comparison of LL-**1** (gray trace) and DD-**1** (black trace) spectra; (b) comparison of LD-**1** (gray trace) and DL-**1** (black trace) spectra. All the spectra were obtained in an aqueous buffered solution (100 mM phosphate buffer, pD 5.8) at 300 K.

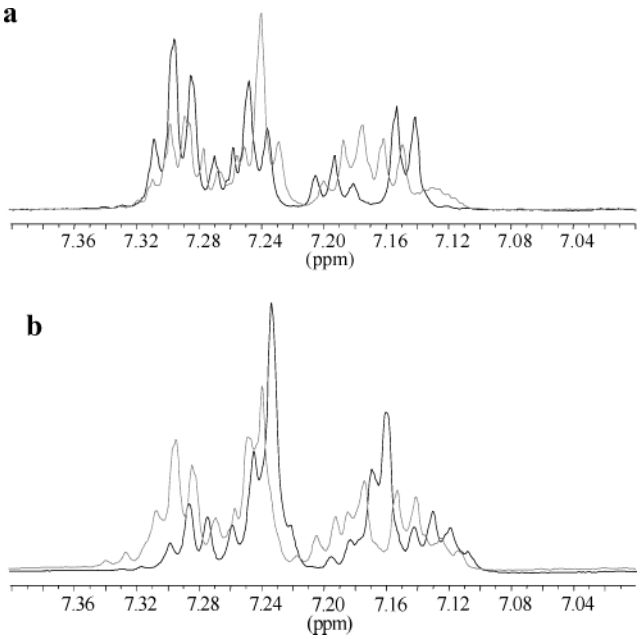

Figure 2. Comparison of the aromatic regions of the 600.13 MHz ^{1}H NMR spectra of 20 mM **2** enantiomers in 94 mM SDP: (a) comparison of LL-**2** (black trace) and DD-**2** (gray trace) spectra; (b) comparison of LD-**2** (black trace) and DL-**2** (gray trace) spectra. All the spectra were obtained in an aqueous buffered solution (100 mM phosphate buffer, pD 5.8) at 300 K.

Scheme 1

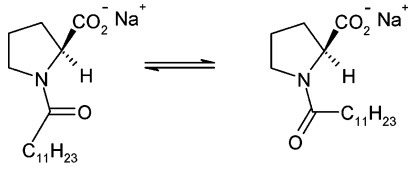

3Z **3E**

where we report the spectrum of the buffered solution of the racemic mixture of LL-**1** and DD-**1** obtained in the presence of SDP aggregates.

The ^{1}H NMR spectra of the dipeptides in the presence of chiral aggregates also allowed us to study the association of **1** and **2** with the chiral aggregates. The chemical shifts of some

(5) (a) Borocci, S.; Mancini, G.; Cerichelli, G.; Luchetti, L. *Langmuir* **1999**, *15*, 2627−2630. (b) Cerichelli, G.; Luchetti, L.; Mancini, G. *Langmuir* **1997**, *13*, 4767−4769.
(6) (a) Belogi, G.; Croce, M.; Mancini, G. *Langmuir* **1997**, *13*, 2903−2904. (b) Bella, J.; Borocci, S.; Mancini, G. *Langmuir* **1999**, *15*, 8025−8031.
(7) Skrabal, P.; Rizzo, V.; Baici, A.; Bangerter, F.; Luisi, P. L. *Biopolymers* **1979**, *18*, 995−1008.
(8) Spectral assignment of diphenylalanine was judged unnecessary for the aim of this study.

Table 1. ^{1}H Spectral Assignment of 20 mM Ditryptophan Diastereoisomers in an Aqueous Buffered Solution (100 mM Phosphate Buffer, pD 5.8) of 94 mM Sodium *N*-Dodecanoyl-L-prolinate

type	δ(LL-**1**) (ppm)	δ(DD-**1**) (ppm)	δ(LD-**1**) (ppm)	δ(DL-**1**) (ppm)
α	3.981	3.987	4.168	4.174
β	3.184	3.179	3.050	3.073
2	7.235	7.222	7.057	7.068
4	7.431	7.458	7.268	7.286
5	6.967	6.973	6.841	6.858
6	7.060	7.064	7.014	7.018
7	7.352	7.355	7.319	7.317
α′	4.378	4.376	4.468	4.454
β′	3.25, 3.13	3.24, 3.13	3.105	3.095
2′	7.124	7.132	7.135	7.125
4′	7.247	7.260	7.408	7.426
5′	6.819	6.807	6.907	6.920
6′	6.977	6.980	6.922	6.996
7′	7.301	7.305	7.319	7.317

resonances of SDP in the spectra recorded in the absence and in the presence of the dipeptides are reported in Table 2. For clarity, the ^{1}H NMR spectrum of a buffered 94 mM SDP solution with the corresponding spectral assignment is reported in Figure 4. Because of the association of **1** isomers with SDP micelles, some ^{1}H resonances due to SDP protons ($\delta_Z{}^{syn}$, $\delta_Z{}^{anti}$, and 1-CH_2) are significantly upfield shifted, while the resonances due to $\delta_E{}^{syn}$ and $\delta_E{}^{anti}$ protons are scarcely affected by the association of **1** isomers. Note that the chemical shift variations of the same resonances, $\delta_Z{}^{syn}$, $\delta_Z{}^{anti}$, and 1-CH_2, due to the association of the isomers of **2** are much smaller than those observed for the isomers of **1**, and similar for the resonances of δ_Z and δ_E protons. These results suggest on one hand a weaker binding of **2** as compared to **1** and on the other a different mode of interaction of the **1** and **2** isomers. In fact, the high extent of chemical shift variation of the resonances of $\delta_Z{}^{syn}$ and $\delta_Z{}^{anti}$ protons implies that **1** isomers bind more specifically to the *Z* domains of the SDP micelles, whereas the lack of this effect shows that the **2** isomers do not feature any specificity of binding. The different chemical shift variation of δ_Z and δ_E protons is clearly evidenced by 2D TOCSY experiments reported in Figure 5 for the LL-**1** and LL-**2** isomers. The selective association of a solute with the *Z* domains of SDP micelles has already been reported in the case of a biphenylic derivative.[4b] This selectivity can be ascribed either to a better fitting of the solute into the grooves formed by the *Z* isomer or to the presence of larger grooves in the domains formed by the *Z* isomer, or both.

From the ^{1}H NMR spectra, differences in the association of homochiral enantiomers (LL and DD) of **1** with respect to heterochiral ones (DL and LD) can also be observed. In fact, Table 2 shows that the association of LL-**1** and DD-**1** with SDP micelles induces a slightly larger upfield shift of the headgroup protons of SDP (α, $\delta_Z{}^{syn}$, $\delta_Z{}^{anti}$) with respect to the shift induced by DL-**1** and LD-**1**. Furthermore, some protons of the aliphatic chain (chain, 11-CH_3) are upfield shifted by the association of heterochiral **1**, whereas the same protons are downfield shifted by the association of homochiral **1**. These observations suggest different sites of binding for homochiral and heterochiral **1**. In

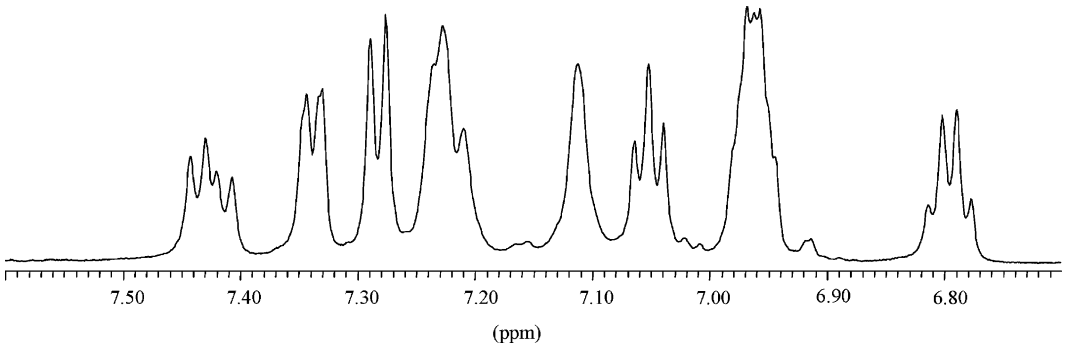

Figure 3. Aromatic region of the 600.13 MHz ^{1}H NMR spectrum of the racemic mixture of LL-**1** and DD-**1** in an aqueous phosphate buffer solution of 94 mM SDP.

Table 2. Chemical Shift Values (ppm) and Chemical Shift Variations (ppm, in Parentheses) of the Resolved Proton Signals of 0.094 M Sodium *N*-Dodecanoyl-L-prolinate in the Absence and in the Presence of 20 mM Dipeptides

	α	$\delta_Z{}^{anti}$	$\delta_E{}^{syn}$	$\delta_E{}^{anti}$	$\delta_Z{}^{syn}$	1-CH_2	2-CH_2	chain	11-CH_3
SDP	4.267	3.706	3.561	3.461	3.431	2.355	1.595	1.293	0.885
SDP + LD-**1**	4.197	3.580	3.547	3.406	3.255	2.236	1.536	1.243	0.883
	(0.070)	(0.126)	(0.014)	(0.055)	(0.176)	(0.119)	(0.059)	(0.050)	(0.002)
SDP + DL-**1**	4.208	3.576	3.549	3.412	3.262	2.231	1.534	1.246	0.883
	(0.059)	(0.130)	(0.012)	(0.049)	(0.169)	(0.124)	(0.061)	(0.047)	(0.002)
SDP + DD-**1**	4.188	3.570	3.550	3.410	3.247	2.227	1.530	1.302	0.917
	(0.079)	(0.136)	(0.011)	(0.051)	(0.184)	(0.128)	(0.065)	(−0.009)	(−0.032)
SDP + LL-**1**	4.167	3.533	3.528	3.389	3.203	2.181	1.499	1.306	0.924
	(0.100)	(0.173)	(0.028)	(0.072)	(0.228)	(0.174)	(0.096)	(−0.013)	(−0.039)
SDP + LL-**2**	4.264	3.702	3.564	3.456	3.420	2.351	1.587	1.300	0.894
	(0.003)	(0.004)	(-0.003)	(0.005)	(0.011)	(0.004)	(0.008)	(−0.007)	(−0.009)
SDP + DD-**2**	4.260	3.701	3.566	3.443	3.417	2.350	1.588	1.296	0.892
	(0.007)	(0.005)	(-0.005)	(0.018)	(0.014)	(0.005)	(0.017)	(−0.003)	(−0.007)
SDP + LD-**2**	4.255	3.693	3.558	3.433	3.405	2.341	1.579	1.284	0.881
	(0.012)	(0.013)	(0.003)	(0.028)	(0.026)	(0.014)	(0.016)	(0.009)	(0.004)
SDP + DL-**2**	4.263	3.698	3.564	3.435	3.411	2.347	1.585	1.284	0.881
	(0.004)	(0.008)	(-0.003)	(0.026)	(0.020)	(0.008)	(0.010)	(0.009)	(0.004)

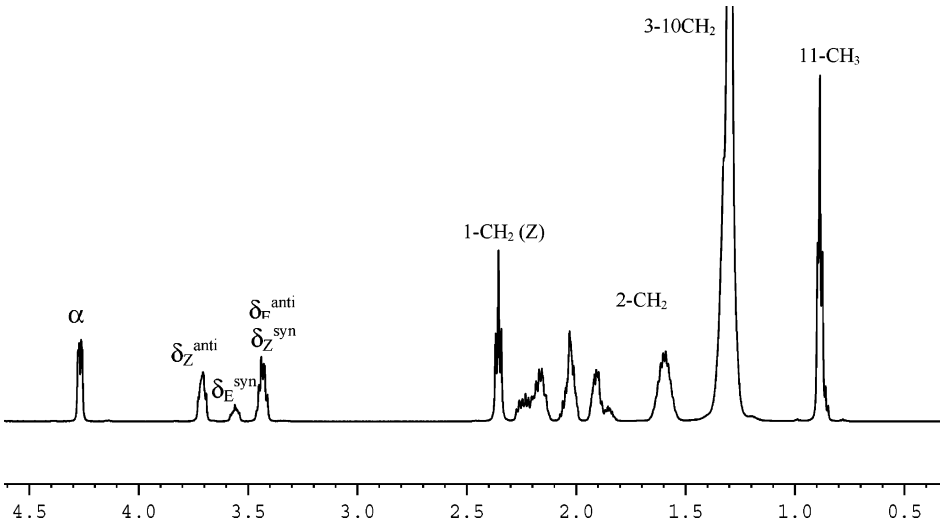

Figure 4. ^{1}H NMR spectrum of 94 mM SDP in an aqueous phosphate buffer solution (100 mM phosphate buffer, pD 5.8).

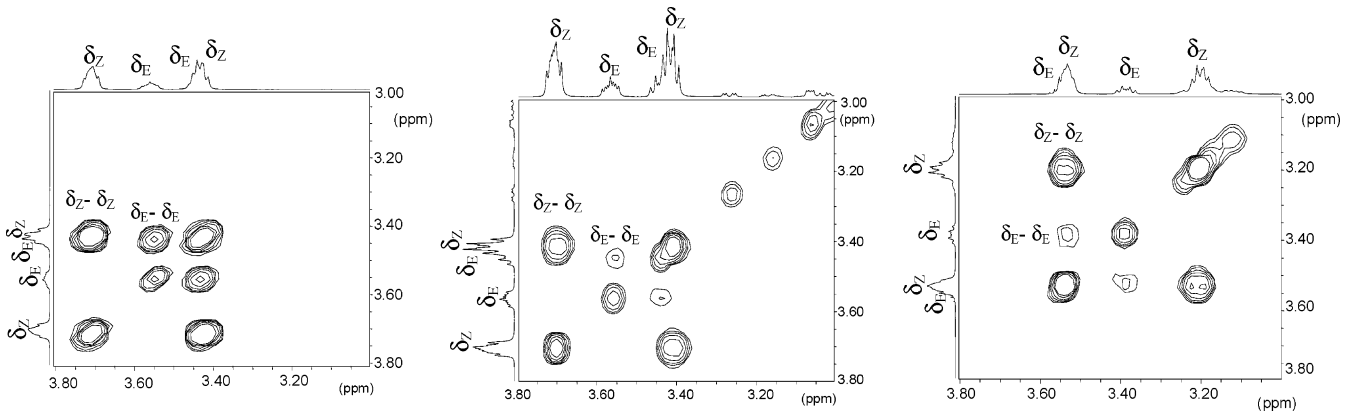

Figure 5. Comparison of the ^{1}H spectral regions relative to pyrrolidinic δ proton signals of aqueous solutions of (left) 94 mM SDP in phosphate buffer solution, (middle) 94 mM SDP and 20 mM LL-**2** in phosphate buffer solution, and (right) 94 mM SDP and 20 mM LL-**1** in phosphate buffer solution.

fact, on one hand, the upfield shift observed for the resonances of the aliphatic chain, as a consequence of the association of the heterochiral isomers of **1**, demonstrates a penetration of the aromatic system in the hydrophobic region of the aggregate as the protons of the aliphatic chain are in the shielding cone of the aromatic system. On the other hand, the downfield shift observed for the same resonances following the association of the homochiral isomers of **1** suggests a site of binding in the headgroup region, as the same protons are in the deshielding cone of the aromatic system. Alternatively, in the case of the association of homochiral isomers the downfield shift observed for the resonances of the aliphatic chain could be explained with a more extended form of the chain.

As expected, a lower concentration of **1** isomers induces a smaller chemical shift variation characterized by an analogous trend. These data are available as Supporting Information (Table 7S).

The partition of **1** and **2** isomers in buffer and in the chiral micellar phase was studied by pulsed-field-gradient NMR (PFG-NMR) experiments.[9] PFG-NMR studies of peptide−micelle interactions have been previously reported.[10] The partition coefficients obtained by PFG-NMR experiments, reported in Table 3, are in good agreement with data reported in the literature for the partition of **1** in water and in sodium dodecyl sulfate micelles determined by UV spectroscopy.[11]

For comparison with other literature data[10a,c] we also report the association constants of dipeptides with the chiral aggregates (Table 3). These constants refer to the equilibrium

$$\text{peptide} + \text{D} \leftrightarrows \text{peptide}\cdot\text{D} \qquad (1)$$

where D is the micellized surfactant whose concentration equals the analytical concentration minus the critical micellar concentration, cmc.

In Table 3 it can be observed that diffusion experiments put into evidence that **1** isomers have a higher affinity for SDP micelles than **2** isomers. This higher affinity, already suggested by the results reported in Table 2, is probably due to the larger aromatic portion of **1** isomers and to their better fitting into the grooves of SDP micelles.

In addition, Table 3 shows that heterochiral dipeptides have a higher affinity for the chiral micellar phase with respect to

(9) (a) Stilbs, P. *Prog. Nucl. Magn. Reson. Spectrosc.* **1987**, *19*, 1−45. (b) Price, W. S. *Concepts Magn. Reson.* **1997**, *9*, 299−336. (c) Galantini, l.; Giampaolo, S. M.; Mannina, L.; Pavel, N. V.; Viel, S. *J. Phys. Chem. B* **2004**, *108*, 4799−4805.

(10) (a) Deaton, K. R.; Feyen, E. A.; Nkulabi, H. J.; Morris, K. F. *Magn. Reson. Chem.* **2001**, *39*, 276−282. (b) Chen, A.; Wu, D.; Johnson, C. S., Jr. *J. Phys. Chem.* **1995**, *99*, 828−834. (c) Orfi, L.; Lin, M.; Larive, C. K. *Anal. Chem.* **1998**, *70*, 1339−1345. (d) Gao, X.; Wong, T. C. *Biophys. J.* **1998**, *74*, 1871−1888.

(11) Iamamura, T.; Konishi, K. *J. Colloid Interface Sci.* **1998**, *198*, 300−307.

Table 3. Dipeptide and Sodium *N*-Dodecanoyl-L-prolinate Aggregate Parameters Obtained by Diffusion Experiments

	D_{free} (10^{-10} m^2 s^{-1})	D_{obs} (10^{-10} m^2 s^{-1})	x_b	D_{obs}(SDP)[a] (10^{-10} m^2 s^{-1})	x_{mic}	p	K (M^{-1})
SDP ([SDP] < cmc)	4.45 ± 0.08						
SDP ([SDP] > cmc)				0.83 ± 0.02	0.99		
LL-**1**	4.43 ± 0.08	0.92 ± 0.01	0.962 ± 0.004	0.83 ± 0.02	0.99	931 ± 100	272 ± 30
DD-**1**	4.43 ± 0.08	0.93 ± 0.01	0.959 ± 0.004	0.83 ± 0.02	0.99	860 ± 87	251 ± 26
DL-**1**	4.43 ± 0.08	0.85 ± 0.01	0.981 ± 0.004	0.84 ± 0.02	0.99	1900 ± 407	554 ± 119
LD-**1**	4.43 ± 0.08	0.85 ± 0.01	0.981 ± 0.004	0.84 ± 0.02	0.99	1900 ± 407	554 ± 119
LL-**2**	4.68 ± 0.06	2.0 ± 0.1	0.69 ± 0.03	0.84 ± 0.02	0.99	82 ± 12	24 ± 4
DD-**2**	4.68 ± 0.06	2.0 ± 0.1	0.69 ± 0.03	0.83 ± 0.02	0.99	82 ± 12	24 ± 4
LD-**2**	4.68 ± 0.06	1.6 ± 0.1	0.79 ± 0.03	0.85 ± 0.02	0.99	138 ± 25	40 ± 7
DL-**2**	4.68 ± 0.06	1.6 ± 0.1	0.79 ± 0.03	0.85 ± 0.02	0.99	138 ± 25	40 ± 7

[a] We used $D_{mic} = (0.78 \pm 0.01) \times 10^{-10}$ m^2 s^{-1} as the value of the diffusion coefficient for micellized surfactant as explained in the Experimental Section.

Table 4. Interproton Distance Obtained from ROESY and NOESY Experiments and Used as Restraints in Molecular Mechanics Calculation

	SDP buffered solution[a]				buffer solution[b]	
proton	LL-**1**	DD-**1**	LD-**1**	DL-**1**	LL-**1**	DL-**1**
β-4[c]	3.0	3.0	2.7	3.0	3.0	2.9
β'-4′	2.7[d]	3.3[d]	2.8[c]	2.9[c]	3.3[d]	3.2[d]
α-4	2.8	3.0		3.1	3.4	3.4
α′-4′	3.6	4.1	3.5	3.4	3.6	3.3

[a] ROESY experiments (20 mM dipeptide and 94 mM SDP in 100 mM phpsphate buffer). [b] NOESY experiments (3.8 mM dipeptide in 100 mM phosphate buffer). [c] The signals due to diastereotopic β (β') protons are coincident. [d] The distance reported is the average of the distances obtained for the diastereotopic β' protons ($\langle r \rangle = \langle r^6 \rangle^{1/6}$; $(1/r^6 + 1/(r')^6)/2 = 1/\langle r^6 \rangle$).

the homochiral isomers, the binding of LD and DL enantiomers being stronger than that of DD and LL enantiomers.

The information obtained by the ^{1}H NMR (Table 2) and diffusion experiments on **1** isomers suggests that, in a dynamic situation, the DL-**1** and LD-**1** isomers penetrate into the hydrophobic part of the aggregates whereas the LL-**1** and DD-**1** isomers bind more specifically to the region close to headgroups of the micellized surfactant. In fact, by comparing the DD/LL and DL/LD couples, we observe a larger upfield shift induced by the homochiral dipeptides on the headgroup signals (Table 2) in correspondence with a lower extent of association (Table 3). The observation of upfield and downfield shifts induced on the ^{1}H resonances of the aliphatic chain by heterochiral and homochiral ditryptophan, respectively (Table 2), strongly supports this hypothesis.

Because of the stronger binding of **1** to SDP micelles with respect to that of **2**, we further investigated only the association of **1** isomers with the chiral SDP aggregates. In particular, to compare the conformation of the four diastereomers of **1** both in the presence and in the absence of chiral aggregates, a conformational search was carried out by means of molecular mechanics calculation using, as distance restraints, the experimental distances reported in Table 4 obtained by ROESY and NOESY experiments.

The obtained conformations are reported in Figure 6, whereas the torsion angles relative to the structures defined by an energy minimum are given as Supporting Information (Table 8S). Figure 6 shows that the conformations of homochiral dipeptides in the chiral aggregates (Figure 6a,c) and in phosphate buffer (Figure 6e) are rather similar; in fact, although some variations in the torsion angles are present, the aromatic portions of the amino acidic residues face each other in both media and the dipeptides show a "folded conformation". Note that, in the

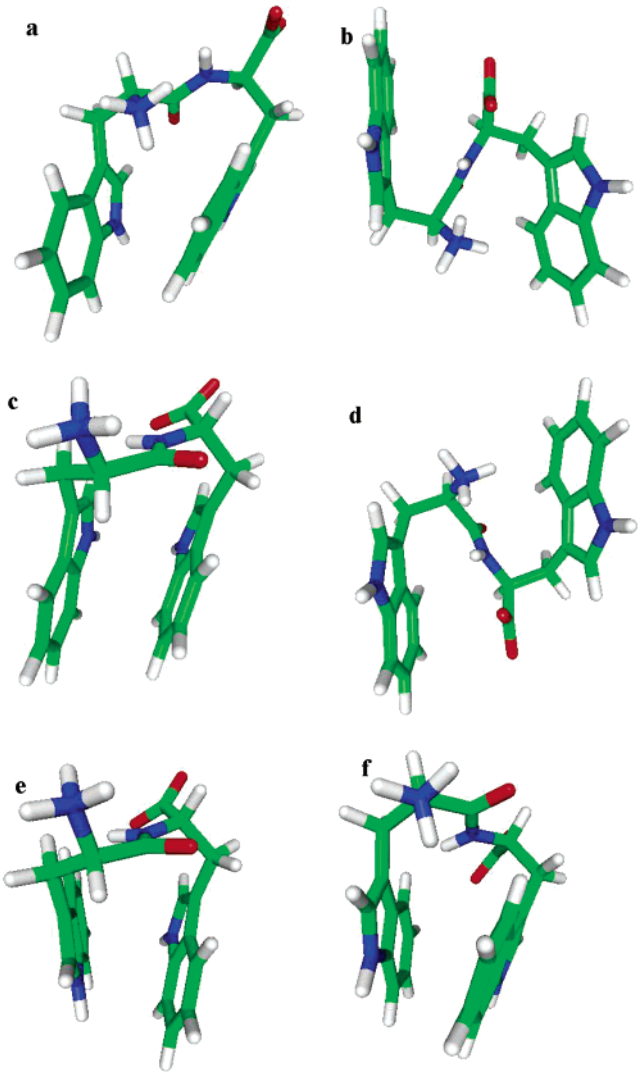

Figure 6. Stick representation of the minimum-energy conformer, obtained by a restrained conformational search, of (a) DD-**1** in SDP, (b) LD-**1** in SDP, (c) LL-**1** in SDP, (d) DL-**1** in SDP, (e) LL-**1** in phosphate buffer, and (f) DL-**1** in phosphate buffer.

conformations obtained in the micellar medium (Figure 6a,c), the indolic nitrogens face each other, whereas, in the conformation obtained in the simple phosphate buffer (Figure 6e), the indolic nitrogens point toward opposite directions. In phosphate buffer, the conformation assumed by heterochiral dipeptides is similar, i.e., "folded", to that of the homochiral isomers (Figure 6f). In contrast, in the chiral aggregates (Figure 6b,d), the

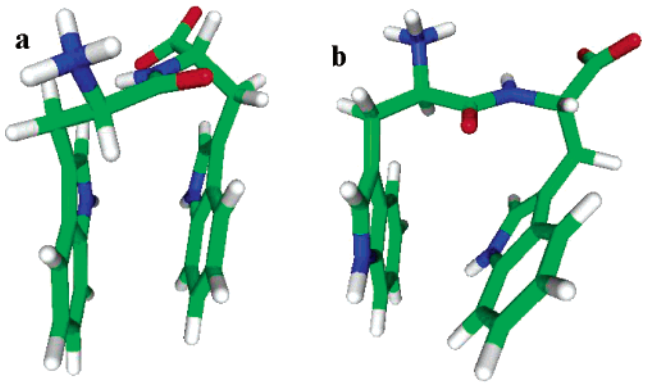

Figure 7. Stick representation of the minimum-energy conformer, obtained by a restrained conformational search, of (a) LL-**1** in SDSR and (b) DL-**1** in SDSR.

conformations are very different; in fact, the aromatic rings of the heterochiral dipeptides do not face each other, and the resulting conformations are "defolded".

A conformational search carried out without distance restraints on LL-**1** and DL-**1** yielded for both isomers folded structures, which we report as Supporting Information (Figure 1S).

With regard to the conformational search results, it is not trivial to understand if the unfolded conformation of heterochiral dipeptides in the chiral aggregates is due to the chiral environment or to the structural features (for example, the anisotropy) of the micellar aggregates.

To clarify this point, we performed diffusion and ROESY experiments on LL-**1** and DL-**1** in aggregates formed by sodium *N*-dodecanoylsarcosinate, SDSR (**4**), which is a "nonchiral" amidic surfactant featuring the same functional groups and the same kind of organization of SDP.[5b] Partition coefficients obtained for LL-**1** and DL-**1** are 1326 ± 202 and 2591 ± 751, respectively (all other parameters relative to the diffusion experiments are reported in Table 9S of the Supporting Information). Therefore, it seems that the different extents of association observed for homochiral and heterochiral dipeptides with SDP are not due to a chiral recognition phenomenon. The dipeptide intramolecular distances obtained by ROESY experiments (reported in Table 10S of the Supporting Information) were used in a conformational search that yielded the minima reported in Figure 7. It can be observed that the conformation of LL-**1** in SDSR micelles (Figure 7a) is folded and substantially similar to that featured in SDP micelles (Figure 6a,c) with the indolic nitrogens facing each other, whereas the conformation of DL-**1** in SDSR micelles (Figure 7b) is slightly more open than that in phosphate buffer (Figure 6f) but is still substantially folded with respect to the conformation obtained in the chiral SDP aggregates (Figure 6b,d).

These results suggest that probably both the chiral and the anisotropic environments of the aggregates are responsible for the different conformations featured by homo- and heterochiral dipeptides in SDP aggregates. In fact, we observed that in SDSR aggregates DL-**1** has an intermediate conformation between those featured in phosphate buffer and in SDP aggregates, respectively.

All these results suggest that micelle-associated homochiral dipeptides show, as reported elsewhere for other hydrophobic dipeptides,[12] two distinct regions: a polar one exposed to the water and a hydrophobic one exposed to the aggregate interior.

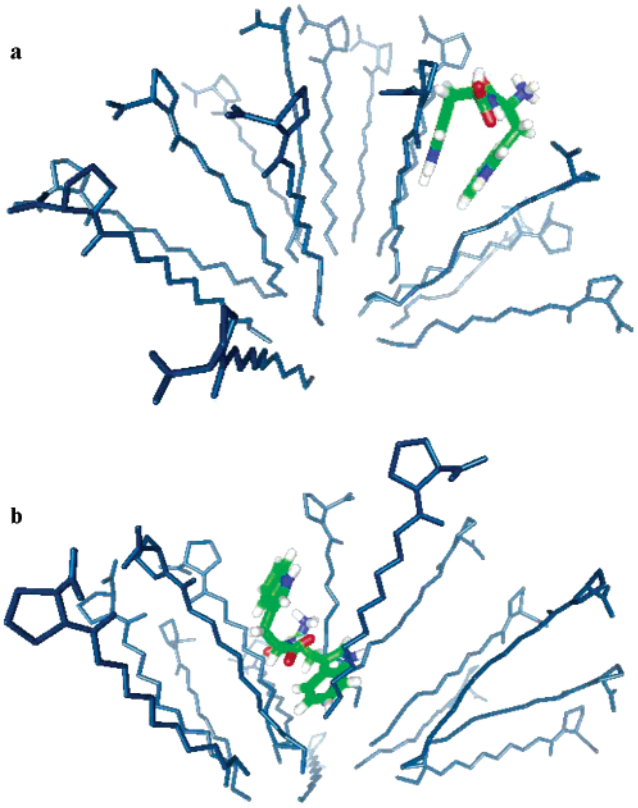

Figure 8. Representation of the different binding modes of (a) homochiral and (b) heterochiral **1** with the micellar aggregates.

In the conformation of heterochiral **1** bound to the chiral aggregates (Figure 6b,d) the polar part is embedded in the hydrophobic part. The SDP aggregates seem to impose a completely different conformation to the heterochiral dipeptides as compared to the homochiral ones. This result is in agreement with the results obtained by 1D NMR recognition experiments and by diffusion experiments. Therefore, the major penetration and higher extent of association of LD-**1** and DL-**1** might be due to their defolded and "thinner" conformation. In Figure 8 we tried to represent, with the limits of a static representation, our hypothesis on the different modes of interaction of homo- and heterochiral **1** isomers with the chiral SDP micelles. Our hypothesis would imply that the observed recognition of LD-**1** and DL-**1** takes place far from the chiral headgroups, in a chiral environment, a "chiral pocket", whose chirality is induced by the headgroups.

Recently, we have reported on the chiral topology of a chiral porphyrin induced by specific interactions with an internal region of aggregates formed by SDP.[13] All the results discussed above support the hypothesis that, in chiral aggregates, chiral recognition may occur in a chiral environment induced in an internal region of the aggregate by remote stereogenic centers. Therefore, chiral recognition in polymolecular aggregates cannot be simply ascribed to non-covalent-specific interactions between the solute and the monomers behaving as single entities; it is more likely

(12) Kloosterman, D. A.; Goodwin, J. T.; Burton, P. S.; Conradi, R. A.; Stockman, B. J.; Scahill, T. A.; Blinn, J. R. *Biopolymers* **2000**, *53*, 396−410.
(13) Monti, D.; Cantonetti, V.; Venanzi, M.; Ceccacci, F.; Bombelli, C.; Mancini, G. *Chem. Commun.* **2004**, 972−973.

due to the aggregate as a whole and in its complexity and can occur in regions of the aggregate quite far from the stereogenic centers.

Experimental Section

Materials. Sodium *N*-dodecanoylprolinate (**3**) was prepared as previously described.[3] Sodium *N*-dodecanoylsarcosinate (**4**) was purchased from Aldrich and purified by means of several crystallizations by MeOH and Et_2O. The four diastereomers of diphenylalanine (**2**) and the LL/DD enantiomeric couple of ditryptophan (**1**) were purchased from Research Plus Inc. and used as such. The other two isomers of **1**, LD-**1** and DL-**1**, were prepared as described below.

Preparation of L,D-H-TrpTrp-OH (LD-1) and D,L-H-TrpTrp-OH (DL-1). A 13 mL sample of methanol was added to 280 mg (0.460 mmol) of (*Z*)-D(L)-Trp-L(D)-Trp-OBzl in a two-necked round-bottom flask. The solution previously flushed with N_2 was flushed gently with H_2 after addition, under nitrogen, of Pd/C (10% of the amount of peptide, w/w). The reaction was monitored by TLC ($CHCl_3$/MeOH, 1/1). After removal of the catalyst by filtration on Celite, the solvent was removed under vacuum to yield 150 mg of the dipeptide. ^{1}H NMR, δ (DMSO): 2.769 (dd, 1H, β, $|^2J_\beta| = 24$ Hz, $^3J_{\alpha H-\beta H} = 9.0$ Hz); 3.134 (dd, 1H, β', $|^2J_{\beta'}| = 20$ Hz, $^3J_{\alpha H-\beta' H} = 5.4$ Hz); 3.158 (dd, 1H, β, $|^2J_\beta| = 24$ Hz, $^3J_{\alpha H-\beta H} = 9.0$ Hz); 3.278 (dd, 1H, β', $|^2J_\beta| = 20$ Hz, $^3J_{\alpha H-\beta' H} = 5.4$ Hz); 3.767 (dd, 1H, α, $^3J_{\alpha H-\beta H} = 9$ Hz); 4.566 (s, 1H, α') 7.018 (t, 1H, 5 or 5′, $J_o = 7.2$ Hz); 7.051 (t, 1H, 5′ or 5, $J_o = 7.2$ Hz); 7.130 (t, 1H, 6 or 6′, $J_o = 7.2$ Hz, $J_m = 1.2$ Hz); 7.148 (t, 1H, 6′ or 6, $J_o = 7.2$ Hz, $J_m = 1.2$ Hz); 7.199 (d, 1H, 2 or 2′, $J = 1.8$ Hz); 7.207 (d, 1H, 2′ or 2, $J = 1.8$ Hz); 7.403 (d, 1H, 7 or 7′, $J_o = 7.2$ Hz); 7.426 (d, 1H, 7′ or 7, $J_o = 7.2$ Hz); 7.641 (d, 1H, 4 or 4′, $J_o = 7.2$ Hz); 7.654 (d, 1H, 4 or 4′, $J_o = 7.2$ Hz); 8.430 (s, 1H, amidic H); 10.909 (d, 1H, 1 or 1′, $J_o = 1.8$); 10.962 (d, 1H, 1 or 1′, $J_o = 1.8$). ^{13}C NMR, δ (DMSO): 174.20, 172.86, 172.85, 137.13, 136.91, 128.36, 128.10, 125.06, 124.48, 121.78, 121.63, 119.36, 119.25, 119.11, 119.08, 112.19, 112.12, 110.90, 110.27, 55.05, 54.28, 30.51, 28.38. Anal. Calcd for $C_{22}H_{22}N_4O_3 \cdot 1.5H_2O$: C, 63.24; N, 13.41; H, 5.99. Found for the DL isomer: C, 63.34; N, 13.13; H, 6.12. Found for the LD isomer: C, 63.28; N, 13.31; H, 6.01.

Preparation of (*Z*)-D(L)-Trp-L(D)-Trp-OBzl. Into a two-necked round-bottom flask equipped with a $CaCl_2$ tube were introduced 100 mg (0.023 mol) of (*Z*)-D(L)Trp-OH (Bachem) and 1.5 mL of freshly distilled CH_2Cl_2. After cooling at 273 K, 34 mg (0.25 mmol) of 1-hydroxybenzotriazole and 48 mg (0.25 mmol) of EDC·HCl were added under stirring. After 30 min 92 mg (0.25 mmol) of H-L(D)-Trp-OBzl (Bachem) was added to the reaction mixture, controlling the pH and keeping it in the range 7−8 by addition of *N*-methylmorpholine. The reaction mixture was stirred for 24 h at room temperature. After removal of the solvent under reduced pressure, the residue was dissolved in 4 mL of ethyl acetate, and the organic solution was sequentially washed with an aqueous solution of 10% $KHSO_4$, with water, and with an aqueous solution of 5% $NaHCO_3$. Removal of solvent under vacuum gave 110 mg (35% yield) of (*Z*)-D(L)-Trp-L(D)-Trp-OBzl, which was determined to be pure by NMR characterization and used as such for the next step. ^{1}H NMR, δ ($CDCl_3$): 2.80−3.30 (m, 4H, β and β'); 4.509 (m, 1H, α'); 4.843 (m, 1H, α); 4.96−5.18 (m, 4H, benzylic methylenes); 5.367 (m, 1H, amidic H); 6.235 (m, 1H, terminal N*H*); 6.330 (d, 1H, 2 or 2′, $J_o = 2.13$ Hz); 6.702 (d, 1H, 2 or 2′, $J_o = 2.13$ Hz); 6.98−7.41 (m, 18H, aromatic H); 7.55−7.74 (m, 2H, 1 and 1′).

Samples. A 100 mM sodium phosphate buffer in D_2O, pD 5.8, was used to prepare all solutions considered in this study. The SDP and SDSR concentration, 94 mM, ensures the predominance of micellar aggregates (10 and 8 mM being the critical micellar concentrations of SDP[5a] and SDSR,[5b] respectively, in the absence of buffer and definitely lower in buffer and in the presence of solutes).

Dipeptide samples were prepared by dissolving the proper amount of **1** and **2** directly into the NMR tubes. The concentration of dipeptide used for most 1D and 2D experiments was 20 mM; it was lowered to 3.8 mM for NOESY, NMR diffusion, and some 1D experiments.

NMR Spectroscopy. NMR spectra were recorded on a Bruker AC 300 P spectrometer operating at 300.13 MHz and on a Bruker AVANCE AQS600 spectrometer operating at 600.13 and equipped with a Bruker multinuclear *z*-gradient inverse probe head capable of producing gradients in the *z* direction with a strength of 55 G cm^{-1}. ^{1}H NMR spectra were referenced with respect to the residual proton signal of D_2O ($\delta = 4.780$ ppm at 300 K). All 1D experiments were performed both with and without suppression of the solvent signal, the solvent suppression being achieved by using either low-power presaturation or WATERGATE.[14] In contrast, in 2D experiments,[15] the solvent signal was always suppressed using WATERGATE.

TOCSY experiments were recorded in the TPPI phase-sensitive mode with a spectral width of 6 kHz in both dimensions, a recycle delay of 2 s, a mixing time of 80 ms, 1K data points in f_2, and 512 increments in f_1. Zero filling in f_1 to 1K real data points and sinusoidal window functions in both dimensions were applied before Fourier transformation. ROESY experiments were performed in the TPPI phase-sensitive mode with a spectral sweep width of 6 kHz in both dimensions, a recycle delay of 2 s, an 80 ms mixing time of on-resonance continuous-wave spin lock at $\gamma(H2) = 5$ kHz, 1K real data points in f_2, and 512 increments in f_1. Zero filling in f_1 to 1K real data points and 90° phase-shifted square sine bell window functions in both dimensions were applied before Fourier transformation.

^{1}H−^{13}C gradient-selected HSQC experiments, with ^{13}C GARP decoupling, were recorded in the echo−antiecho phase-sensitive mode by using a selected heteronuclear scalar coupling constant of $^1J_{C-H} = 150$ Hz and the following parameters: a spectral width of 6 kHz in f_2 and 20 kHz in f_1, 1024 data points in f_2, 512 increments in f_1, and a recycle delay of 1 s. The data were processed with a sine bell window function and a 512 × 512 data matrix size.

^{1}H−^{13}C gradient-selected HMBC experiments were recorded in the magnitude mode with a low-pass filter of 3.57 ms and a delay for evolution of 80 ms. The following parameters were also used: a spectral width of 6 kHz in f_2 and 30 kHz in f_1, 1024 data points in f_2, 512 increments in f_1, and a recycle delay of 1 s. The data were processed with a sine bell window function and a 512 × 512 data matrix size.

Determination of Dipeptide Intramolecular Distances. Interproton distances were obtained by the intensity of cross-peaks in ROESY spectra using eq 2,[16]

$$r_{ij} = r_{ref}\left(\frac{I_{ref}c_{ref}}{I_{ij}c_{ij}}\right)^{1/6} \quad (2)$$

where r_{ij} and I_{ij} are the distance and the cross-peak intensity between protons *i* and *j*, respectively, r_{ref} and I_{ref} are the reference distance and the intensity of the reference cross-peak, respectively, and c_{ij} and c_{ref} are the correction factors that take into account the offset dependence of the spin-lock frequency;[16] they were not used in the calculation of distances from NOESY experiments.

The reference distance used in the ROESY experiments is the distance between the $\delta_Z{}^{syn}$ and $\delta_Z{}^{anti}$ protons, because they are nondegenerate and their internuclear distances will be independent of the conformation of the pyrrolidinic ring.[17] The $\delta_Z{}^{syn}$ and $\delta_Z{}^{anti}$ distance, 1.76 Å, was obtained by ab initio HF/6-31G* calculation in a vacuum on the *N*-acetyl-L-prolinate anion.[18] To check the reliability of distances obtained by ROESY experiments, we estimated by ab initio HF/6-31G* calculation the distance between two aromatic protons in *ortho* positions,

(14) Piotto, M.; Saudek, V.; Sklenár, V. *J. Biomol. NMR* **1992**, *2*, 661−665.
(15) Braun, S.; Kalinowski, H.-O.; Berger, S. *150 and more basic NMR experiments: a practical course*; Wiley-VCH: Weinheim, Germany, 1998.
(16) Amälahti, E.; Bardet, M.; Molko, D.; Cadet, J. *J. Magn. Reson., A* **1996**, *122*, 230−232.
(17) Patel, A. B.; Srivastata, S.; Phadke, R. *Magn. Reson. Chem.* **1998**, *36*, 815−825.
(18) Spartan 5.01, Wavefunction, Inc., 18401 Von Karman Ave., Suite 370, Irvine, CA 92612.

namely, the distance between protons in the 4′ and 5′ positions, and compared it with values obtained by ROESY experiments. The calculated (2.45 Å) and experimental (2.6 Å) distances of the protons in *ortho* positions are in good agreement.

The reference distance used in the NOESY experiments is the distance between protons in the 4 and 5 and 4′ and 5′ positions (*ortho* positions), which we set as 2.5 Å.

Molecular Modeling. Molecular mechanics calculations were performed with the MacroModel 6.0 package[19] running on a Silicon Graphics O2 R10000 workstation and using an AMBER* force field.[20] The electrostatic interactions were evaluated by using the partial atomic charges of the AMBER* force field; dielectric constants of 10 and 78 were used to reproduce the micellar[21] and the aqueous media, respectively.

A conformational search with distance restraints was carried out on the molecular structures of the four stereoisomers of ditryptophan using the low-mode conformational search (LMCS) procedure[22] (10000 steps of Monte Carlo simulation each run). The generated structures were energy minimized to a gradient lower than 0.001 kJ $mol^{-1}Å^{-1}$ using the Polak−Ribiere conjugate gradient method; an energy window of 25 kJ mol^{-1} above the global minumum was used. The intramolecular hydrogen distances obtained from ROESY experiments were used as restraints in the conformational search and were imposed by using the FXDI command in BatchMin.

All structures found by the restrained search were energy reminimized without restraints to a gradient lower than 0.0001 kJ mol^{-1} $Å^{-1}$ by using the TNGC method.[23]

A conformational search in phosphate buffer solution was performed on LL- and DL-ditryptophan without distance restraints.

PFG-NMR Diffusion Experiments. The self-diffusion coefficients of **1** and **2** were monitored by PFG-NMR experiments. The stimulated-echo sequence incorporating bipolar gradient pulses and a longitudinal eddy current delay (BPP-LED)[24] was used, and when necessary, the HOD residual signal was suppressed by means of a low-power presaturation. In the BPP-LED experiment, the amplitude of an NMR signal observed at the echo is given by[25]

$$I = I_0 \exp\left(-D(\gamma g \delta)^2\left(\Delta - \frac{\delta}{3} - \frac{\tau}{2}\right)\right) \quad (3)$$

where I_0 is the resonance amplitude at zero gradient strength, γ is the magnetogyric ratio of the proton, g, δ, and Δ are the strength, the duration, and the separation of the gradient pulses, respectively, and τ is equal to the gradient pulse recovery time. The gradient strength was logarithmically incremented in 16 steps from 2% to 95% of the maximum gradient strength. Diffusion times and gradient pulse durations were optimized for each experiment to achieve a 95% decrease in the resonance intensity at the largest gradient amplitude; typically, diffusion times between 150 and 600 ms and bipolar sine gradient pulses between 1.0 and 1.6 ms were employed. The longitudinal eddy current delay was held constant at 25 ms, whereas the gradient pulse recovery time was set to 0.1 ms. After Fourier transformation and phase correction, the baseline of the spectra was carefully adjusted. The data were analyzed by plotting the signal intensities (areas) as a function of the gradient strength and fitting the resulting decay curves to eq 3 with a nonlinear least-squares fit (Simplex algorithm). All decays were monoexponential,[9a] and the plots of the logarithm of the NMR signal intensity against the square of the gradient strength always gave straight lines.[26]

Determination of Dipeptide Partition from Diffusion Experiments. The analysis of PFG-NMR data is based on a two-site model, assuming the dipeptide to be in equilibrium between the aqueous (free) and the micellar (bound) phases. If the equilibrium is fast with respect to the NMR and diffusion time scales, then the observed diffusion coefficient of the dipeptides is given by[9a,27]

$$D_{obs} = x_b D_b + (1 - x_b) D_f \quad (4)$$

where D_b and D_f refer to the diffusion coefficients of the bound and free dipeptides, respectively, and x_b is the molar fraction of the bound dipeptides. D_{obs} is obtained by measuring the diffusion coefficient of the dipeptide in the dipeptide/surfactant solution. D_b is considered to be equal to the diffusion coefficient of the micelles, D_{mic}.[27] However, because both micellar and monomeric surfactant molecules undergoing fast chemical exchange are present in the dipeptide/surfactant solution, D_{mic} does not equal the measured diffusion coefficient of the micelles. Therefore, to determine the true D_{mic} value, a hydrophobic probe is added in a trace amount to the dipeptide/surfactant solution. Here we chose hexamethyldisilane (HMDS),[9a,10d] and the following value was found: $D_{mic} = (0.78 \pm 0.01) \times 10^{-10}$ m^2 s^{-1}. D_f was obtained by measuring the diffusion coefficient of the dipeptide in a buffered D_2O solution at the same concentration as that used in the dipeptide/surfactant solution (3.8 mM). The diffusion coefficient of a small noninteracting molecule, β-mercaptoethanol at 10 mM, was also measured in buffered D_2O and 94 mM SDP solution to ascertain that, in our experimental conditions, obstruction effects and viscosity changes were negligible.[10a−c]

The previously mentioned partition equilibrium can be characterized by a partition coefficient p defined as the ratio of the dipeptide concentrations in the micellar and aqueous phases, that is[27]

$$p = \frac{x_b}{(1 - x_b)} \frac{V_{aq}}{V_{mic}} \quad (5)$$

where V_{aq} and V_{mic} are the volumes of the aqueous and micellar phases, respectively; their ratio was estimated by their respective weight fractions.[10d]

The association constant, K, relative to equilibrium 1, was calculated according to[10a,c]

$$K = \frac{[DP]_{bound}}{[DP]_{free}[SDP]_{mic}} \quad (6)$$

where [DP] is the concentration of the dipeptides in the respective phases, and $[SDP]_{mic}$ is the concentration of micellized surfactant molecules. Equation 6 can be rearranged to

$$K = \frac{x_b}{(1 - x_b) x_{mic} [SDP]_0} \quad (7)$$

where $[SDP]_0$ is the SDP analytical concentration and x_{mic} is the fraction of micellized surfactant obtained by the diffusion coefficients of free surfactant, D_f, and of the aggregates, D_{mic}, and by the diffusion coefficient observed in aggregating conditions, D_{obs}(SDP).[10c] D_f(SDP) was obtained by a separate PFG-NMR experiment performed on a buffered 1 mM SDP solution, i.e., well below the SDP cmc (10 mM in pure D_2O).

Conclusions

The interaction between chiral micellar aggregates formed by **3** and the four diastereomers of **1** and **2** was investigated by

(19) Mohamadi, F.; Richards, N. G. J.; Guida, W. C.; Liskamp, R.; Lipton, M.; Caufield, C.; Chang, G.; Hendrikson, T.; Still, W. C. *J. Comput. Chem.* **1990**, *11*, 440−467.
(20) (a) Weiner, S. J.; Kollman, P. A.; Case, D. A.; Singh, U. C.; Ghio, C.; Alagona, G.; Profeta, S., Jr.; Weiner, P. *J. Am. Chem. Soc.* **1984**, *106*, 765−784. (b) McDonald, D. Q.; Still, W. C. *Tetrahedron Lett.* **1992**, *33*, 7747−7750.
(21) (a) Bunton, C. A.; Minch, M. J.; Hildago, J.; Sepulveda, L. *J. Am. Chem. Soc.* **1973**, *95*, 3262−3272. (b) Carpenter, K. A.; Wilkes, B. C.; Weltrowska, G.; Schiller, P. W. *Eur. J. Biochem.* **1996**, *241*, 756−764.
(22) Kolossváry, I.; Guida, W. C. *J. Am. Chem. Soc* **1996**, *118*, 5011−5019.
(23) Ponder, J. W.; Richards, F. M. *J. Comput. Chem.* **1987**, *8*, 1016−1024.
(24) Wu, D.; Johnson, C. S., Jr. *J. Magn. Reson.* **1995**, *115*, 260−264.
(25) Stejskal, E. O.; Tanner, J. E. *J. Chem. Phys.* **1965**, *42*, 288−291.
(26) Chen, A.; Shapiro, M. J. *J. Am. Chem. Soc.* **1999**, *121*, 5338−5339.
(27) Stilbs, P. *J. Colloid Interface Sci.* **1982**, *87*, 385−394.

NMR spectroscopy. Our results evidenced chiral recognition of the enantiomeric couples of the dipeptides and markedly different extents of association of **1** and **2**. We could not observe enantioselectivity in the association with the chiral aggregates, whereas we evidenced some differences in the extent and in the mode of association of the homochiral diastereomers of **1** with respect to the heterochiral ones, though these seem not completely due to the chiral environment of the aggregates. The differences concern a higher extent of association of heterochiral diastereomers with respect to homochiral diastereomers, different conformations, folded for homochiral **1** and defolded for heterochiral **1**, and different sites of binding. The chemical shift variations of the SDP resonances suggest, in fact, that LD-**1** and DL-**1** are associated with a more internal region of the aggregate with respect to LL-**1** and DD-**1**; the evidence of different conformations supports this result. The proposed model of interaction implies that chiral recognition occurs, in the case of heterochiral dipeptides, in a region far from the stereogenic centers.

These results confirm that chiral recognition in biological membranes is a complex process that may also occur in internal regions of the lipid double layer, i.e., far from the stereogenic centers.

Because of the high organization observed in a simple system such as the model we have investigated, we believe that it is reasonable to investigate the role of more organized systems, such as primordial biomembranes, in the homochirality of biopolymers. Although the micellar aggregates considered as a model in this study are formed by a surfactant whose structure does not resemble membrane phospholipids, the interactions involved are very similar to those involved in a more complex and organized aggregate. The amide bond is, in fact, characteristic of sphingolipids, which, being among the main components of biomembranes, feature the phosphate group only in the case of sphingomyelins. Moreover, the components of primordial biomembranes were possibly different from today's phospholipids,[2c] and any type of aggregate of amphiphilic molecules might have acted as a primordial biomembrane.

The investigations on chiral recognition in self-aggregated systems are also of importance in a wider context and scope, because they may clarify the interactions involved in the transfer of chirality from the molecular to a higher level of complexity.

Acknowledgment. This work has been carried out in the frame of the project "the use of surfaces and vesicles for the amplification of homochirality in polypeptide chains" of COST action D27 (prebiotic chemistry and early evolution).

Supporting Information Available: ^{1}H and ^{13}C spectral assignments of 3.8 mM ditryptophan diastereoisomers in 100 mM phosphate buffer (pD 5.8) in the absence and in the presence of chiral micellar aggregates, chemical shift values of the proton signals of sodium *N*-dodecanoylprolinate in the absence and in the presence of 3.8 mM ditryptophan diastereomers, torsional angles of low-energy conformers of ditryptophan diastereoisomers obtained from molecular mechanics calculation, ditryptophan and SDSR aggregate parameters obtained by diffusion NMR experiments, ditryptophan interproton distances obtained from ROESY experiments performed in the presence of 94 mM SDSR, and stick representation of the minimum-energy conformer of homo- and heterochiral ditryptophan obtained by an unrestrained conformational search (PDF). This material is available free of charge via the Internet at http://pubs.acs.org.

JA0470057